Shock Relaxation in a Particle-Gas Mixture with Mass Transfer between Phases

RONALD PANTON*
Oklahoma State University, Stillwater, Okla.

AND

A. K. OPPENHEIM†
University of California, Berkeley, Calif.

Structure of the relaxation zone behind a shock front propagating into a particle-gas mixture has been studied for the case where the particles are liquid drops and mass transfer therefore had to be taken into account. After a general formulation of the problem, several computer solutions were obtained under the assumption that the mass transfer is diffusion controlled. All solutions are presented in a general form that is relatively independent of the viscosity-radius parameter. Three topics are presented. The first, a parametric study for single-size particles, brings out the influence of the heat of vaporization, the initial vapor concentration, and the particle loading factor on the gas mass flow rate, and gas and particle velocity and temperature profiles. The second is an investigation of the gas temperature behavior, emphasizing the relative effects of mass transfer, heat transfer, drag, and compression work on the temperature profile. The last topic is a study for the case of two particle sizes yielding the profiles of mass flow rates, velocities, and temperatures of each constituent. An interesting example is presented where the small particles vaporize while the large particles are growing.

Nomenclature

a = speed of sound
c = concentration, moles per unit volume
C_d = drag coefficient
c_p = specific heat at constant pressure
C_p = $c_p/(\gamma_0 R_0)$, nondimensional specific heat
D_{AB} = binary diffusion coefficient
f = drag force per unit volume
F = $f\rho_L r_0/(a_0\rho_{g0})^2$, nondimensional drag
h = specific enthalpy
h_q = heat-transfer coefficient
h_{fg} = heat of vaporization
H = h/a_0^2, nondimensional enthalpy
H_{fg} = h_{fg}/a_0^2, nondimensional heat of vaporization
H_{fg}^0 = H_{fg} at temperature T_0
I = nondimensional constant, see Eq. (1b)
J = nondimensional constant, see Eq. (1c)
k_x = mass transfer coefficient
M = shock Mach number based on a_{g0}
Nu = $h_q 2r/k$, Nusselt number
Nu_D = $k_x 2r/(cD_{AB})$ Nusselt number for mass transfer
p = pressure
p_A, p_B = partial pressure
P = $p/(\rho_{g0}a_0^2)$, nondimensional pressure
Pr = Prandtl number
q = Heat-transfer rate per unit volume
Q = $q\rho_L r_0/(a_0^3\rho_{g0}^2)$, nondimensional heat transfer
r = particle radius
R = r/r_0, nondimensional particle radius
R_0 = universal gas constant
Re = $\rho_g 2r|v_g - v_p|/\mu$, particle Reynolds number
Sc = $\mu/(\rho_{g0}D_{AB})$, Schmidt number
T = temperature
v = velocity
V = v/a_0, nondimensional velocity
w = mass flow rate
W = $w/(\rho_{g0}a_0)$, nondimensional mass flow rate
W^* = W_g/W_{g0}, normalized mass flow rate
X = $x\rho_{g0}/(r_0\rho_L)$, nondimensional distance
X^* = $X(\mu^*)^{1/2}$, nondimensional distance
x_A, x_B = mole fraction
α = σ_1/σ, group loading factor for particles in size group 1
γ = specific heat ratio
δ = σ/ρ_{g0}, particle loading factor
θ = T/T_0, nondimensional temperature
k = thermal conductivity
μ = viscosity
μ^* = $\mu/(r_0 a_0 \rho_{g0})$, nondimensional viscosity
ρ = density of homogeneous substance
ψ = mass transfer rate per unit volume
Ψ = $\psi\rho_L r_0/(a_0\rho_{g0}^2)$, nondimensional mass transfer rate
σ = mass of particles per unit volume of mixture
σ_1 = mass of particles of size group 1 per unit volume of mixture

Subscripts

A, B = chemical species A or B
g = gas phase
L = liquid material
p = particle phase
S = particle surface
0 = initial and reference state before the shock wave
1 = state immediately behind the shock
∞ = equilibrium state far downstream

Introduction

THE flow of a gas containing small droplets or particles has become of importance to a wide range of technological applications in the chemical industry, aeronautics, and rocketry. In general, the two phases are not initially in equilibrium with respect to velocity, temperature, or composition. Equilibrium tends to be restored by the relatively slow processes of drag, heat, and mass transfer as the flow proceeds through a relaxation zone. Of specific interest here is the analysis of the relaxation occurring in a dispersion of liquid droplets in a gas from the nonequilibrium state brought about by a shock wave.

In recent years similar problems have been treated by several authors. Hoenig[1] discussed the behavior of the velocity of a single solid particle behind a shock wave. Car-

Received November 15, 1967; revision received June 5, 1968. This work was supported by NASA under Grant Number NsG-702/05-003-050.

* Assistant Professor, School of Mechanical & Aerospace Engineering. Member AIAA.
† Professor, Division of Aeronautical Sciences. Fellow AIAA.

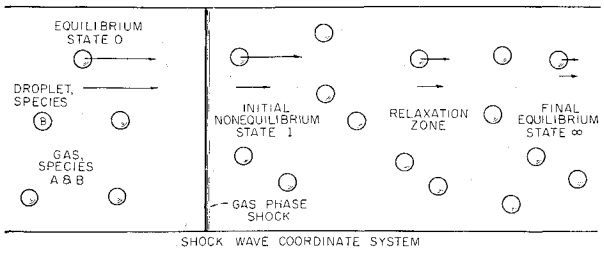

Fig. 1 Physical problem.

rier[2] formulated the general problem for solid particles which are numerous enough to affect the gas flow behind the shock. Rudinger[3] studied numerically the case for solid particles where he varied shock strengths, drag laws, and specific heats. He pointed out that the velocities and temperatures do not always change monotonically toward their equilibrium values. Almost simultaneously, Kriebel[4] gave an approximate analytical solution for weak shock waves and computer results for strong shocks where three particle sizes were present. The only investigation, taking into account mass transfer between phases, has been carried out recently by Lu and Chiu[5] for the case of water droplets in air.

The objective of our work is to study the general nature of the relaxation zone as it is influenced by various parameters, but with particular attention directed towards the effect of mass transfer. Our work, which was started independently and simultaneously with that of Lu and Chiu, can be looked upon as the generalization of their investigation, covering a variety of substances and based on more generally applicable rate laws.

The results showed that in certain instances, the gas temperature dipped below the particle temperature and then rose to a higher value before the equilibrium temperature was attained. This behavior was rationalized and verified by performing a separate computation where each physical phenomenon contributing to changes in the gas temperature was computed. In addition, considered also in our study was the case of two droplet-size groups. This demonstrated the interesting possibility of a situation where some particles diminish by vaporization while others grow by condensation.

Problem Formulation

Basically, the problem concerns a one-dimensional, steady flow of dispersed liquid particles in a gas. Initially, the gas and particles are at given states, but they are not in equilibrium and they move at different velocities. The mixture proceeds to its final equilibrium state by a relaxation process where the two phases interact. The initial state can be specified arbitrarily and then the gas and particle properties computed in the relaxation zone using distance as the independent variable.

Physically, several situations might be imagined which would produce the initial nonequilibrium state: the acceleration of a mixture to the entrance of a pipe, the injection of droplets into a flowing gas stream, or the support of the particles by a screen as in a fluidized bed. Here we assume the initial conditions are produced by a shock wave in the gas phase.

Viewed from a coordinate system on the shock wave, the particles and gas approach with the same supersonic velocity (Fig. 1). The particles, which are much more dense than the gas, penetrate the gas shock because of their high momentum. Likewise, the heat-transfer and mass transfer rates are slow and the particles leave the gas shock unaltered in mass, temperature, or velocity. The gas shock wave, on the other hand, is assumed to be unaffected by the presence of the particles.

The gas phase consists of two chemical species: a diluent A which is insoluble in the liquid, and the droplet vapor denoted by B. The gas phase will be treated as a perfect gas mixture. Upstream of the shock, the phases are assumed to be in equilibrium; therefore, the partial pressure of species B in the gas phase is the saturation pressure corresponding to the droplet temperature. After passing through the shock, the droplet temperature and, hence, the pressure of species B at the surface are unchanged. On the other hand, the vapor of species B in the gas phase has been compressed by the shock to a much higher partial pressure. This partial pressure (or mole fraction) gradient between the main gas stream and the particle surface causes diffusion of species B to the surface of the particle where condensation occurs. The major assumption of our analysis is that diffusion is the rate-controlling mass transfer process. This is true if the rate of condensation (or vaporization) is much faster than the diffusion rate. The droplet rapidly supplies or consumes species B so that the partial pressure of species B at the surface is always in equilibrium with the liquid (as determined by the liquid temperature).

The preceding physical argument shows that immediately behind the shock, the gas phase will condense and the droplets will grow. The condensation of species B is only the initial behavior. Frequently, but not always, vaporization occurs further on the relaxation zone. Lu and Chiu[5] state that condensation may or may not occur immediately behind the shock. This is not contradictory with our conclusion since they allow the flow upstream of the shock to be a nonequilibrium state where the partial pressure of species B in the gas phase is not the equilibrium value.

The algebraic formulation involves six major dependent variables. For each phase, the mass flow rate, velocity, and temperature are nondimensionalized as follows:

$$W_g = \rho_g v_g/(\rho_{g0}a_0) \qquad V_g = v_g/a_0 \qquad \theta_g = T_g/T_0$$
$$W_p = \sigma_p v_p/(\rho_{g0}a_0) \qquad V_p = v_p/a_0 \qquad \theta_p = T_p/T_0$$

Once these variables are known as a function of X, the distance through the relaxation zone, any other property may be found by simple algebra.

The conservation equations for the over-all gas-particle mixture are[2-7]:

$$W_g + W_p = \text{const} = M(1 + \delta) \tag{1a}$$

$$W_g V_g + W_p V_p + P = \text{const} = I \tag{1b}$$

$$W_g(H_g + \tfrac{1}{2}V_g^2) + W_p(H_p + \tfrac{1}{2}V_p^2) = \text{const} = J \tag{1c}$$

In these equations, H is the enthalpy, P the pressure, M the shock Mach number, and δ the loading factor ($\delta = \sigma/\rho_{g0}$). If the particles consist of more than one size group, then the equations are modified accordingly.

Equations governing the particle phase contain sourcelike terms accounting for the interaction with the gas phase:

$$dW_p/dX = -\Psi \tag{2a}$$

$$W_p(dV_p/dX) = F \tag{2b}$$

$$W_p(dH_p/dX) = -\Psi H_{fg} + Q \tag{2c}$$

The symbol Ψ indicates the rate at which mass is exchanged between the phases, F the drag force, and Q the heat transfer. The equations are valid for a dilute mixture where the volume of the particles is a small fraction of the total volume. Some authors have erroneously added terms in Eq. (2b) for a momentum effect of the condensing or vaporizing mass. A careful discussion of this point is given in Ref. 6.

The drag and heat-transfer terms are given by the expression which introduce the drag coefficient C_d and the Nusselt number Nu:

$$F = 3W_g W_p C_d|V_g - V_p|(V_g - V_p)/(8RV_gV_p) \tag{3a}$$

$$Q = 3W_p\mu^* C_{pg}Nu\,(\theta_p - \theta_g)/(2R^2Pr) \tag{3b}$$

For a dilute flow, it seems reasonable to evaluate C_d and Nu

as for a single particle in an infinite gas. Rudinger[8] has given preliminary results showing that the drag coefficient in this unsteady situation differs substantially from previous correlations. He has also shown that the drag law has a strong effect upon the solutions for solid particles.[3] One can expect similar effects associated with the Nusselt numbers, indicating a need for experimental investigation of these parameters. Consequently, with the clear understanding that our solutions can be trusted to be only qualitatively correct until experimental verification of these parameters, we assume

$$C_d = 0.48 + 28\,Re^{-0.85} \tag{4a}$$

$$Nu = 2 + 0.6Re^{1/2}Pr^{1/3} \tag{4b}$$

These are typical expressions valid for a wide range of Reynolds numbers in steady flow.

The mass transfer function was formulated for a diffusion controlled process at a low transfer rate:

$$\Psi = 3W_p\mu^*Nu_D(x_{BS} - x_{Bg})/[2R^2ScV_p(1 - x_{BS})] \tag{5}$$

The term $(1\text{-}x_{BS})$ accounts for bulk flow away from the particle. There is not a uniform practice in defining mass transfer coefficients, and in Eq. (5) we have followed the recommendations of Bird, Stewart, and Lightfoot.[9] They also give a simple correction to extend the results to high transfer rates. The Nusselt number for diffusion was evaluated from Eq. (4b) invoking the heat-mass transfer analogy. Equation (5) differs slightly from the formula used initially by Lu and Chiu.[5] Lu and Chiu found that their droplet temperatures became so high that the partial pressure of the liquid was unrealistically above the gas phase pressure. They attributed this to the low transfer rate limitation on their mass transfer equation and proposed a modification which avoided this difficulty. We did not encounter any problems with our use of Eq. (5).

The thermodynamic equations are written for a perfect gas mixture of species with the same molecular weights:

$$P = W_g\theta_g/(\gamma_0 V_g) \tag{6a}$$

$$x_A = P_A/P = 1 - x_B \tag{6b}$$

$$H = x_AH_A + x_BH_B \tag{6c}$$

$$H_p = C_{pL}(\theta_p - 1) \tag{6d}$$

$$H_A = C_{pA}(\theta_g - 1) \tag{6e}$$

$$H_B = C_{pB}(\theta_g - 1) + H_{fg}^0 \tag{6f}$$

$$H_{fg} = H_{fg}^0 + (C_{pB} - C_{pL})(\theta_p - 1) \tag{6g}$$

Conservation of the diluent, species A, allows the mole fraction to be related to the mass flow rate of gas:

$$x_A = x_{A0}W_{g0}/W_g = (1 - x_{B0})M/W_g \tag{7}$$

It is also assumed that the particles do not break up so the particle radius can be related to the mass flow rate also:

$$R = (W_p/W_{p0})^{1/3} = (W_p/M\delta)^{1/3} \tag{8}$$

The vapor pressure of species B at the particle surface (and therefore the mole fraction x_{BS}) is given by the Clausius-Clapeyron equation:

$$dP_{BS}/d\theta_p = P_{BS}H_{fg}\gamma_0/\theta_p^2 \tag{9}$$

With H_{fg} given previously, this can be integrated to the form

$$P_{BS}/P_{B0} = \exp[H_{fg}^0\gamma_0(1 - \theta_p^{-1})]\cdot K \tag{9a}$$

where K represents a term correcting for the variation of H_{fg} with temperature. K was carried along and used in all the calculations; however, in retrospect it differed only slightly from one and was an unnecessary refinement. The Lu and Chiu analysis differed from ours on this point also; they used an approximate equation, containing the cube of the temperature, which was specifically developed for water.

The preceding set of equations completely determines the problem. The independent parameters that enter the equations are Pr, Sc, C_{pA}, C_{pB}, C_{pL}, H_{fg}^0, x_{BO},δ,μ^*. The initial mole fraction x_{BO} is used to find the reference partial pressure in Eq. (9a). The loading factor δ is the initial ratio of particle material to gas in a unit volume of mixture. It is also the ratio of initial mass flow rates since the velocities of both phases are initially equal. The group μ^* will be called the viscosity-radius parameter:

$$\mu^* = \mu/\rho_{g0}a_0r_0 \tag{10}$$

The size of the particles enters the problem only through this parameter and the nondimensional distance scale. The viscosity-radius parameter can also be interpreted as the inverse of a Reynolds number for the problem. The speed of sound was chosen as the characteristic velocity for the problem and so it appears in the characteristic Reynolds number.

The initial conditions are those immediately behind a gas shock wave. Let 0 and 1 denote the conditions on either side of the shock; then all the following can be found from a shock table once γ_0 and M are chosen:

$$\begin{aligned} &V_p(0) = M \qquad \theta_p(0) = 1 \qquad W_p(0) = M\cdot\delta \\ &V_g(0) = (v_1/v_0)M \qquad \theta_g(0) = T_1/T_0 \qquad W_g(0) = M \end{aligned} \tag{11}$$

Choosing values of the parameters and the Mach number of the shock allows the relaxation zone structure to be computed.

Results

The problem, as formulated in the previous section, has been solved numerically for several cases.[10] The results presented here concern the following specific topics: 1) Parametric study for the case of single particle size, bringing out the relative influence of the heat of evaporation H_{fg}^0, the mole fraction of vapor in the undisturbed mixture x_{B0}, and the particle loading factor δ on the structure of the relaxation zone. 2) Investigation of the gas temperature behavior, analyzing the relative effects of mass transfer, heat transfer, drag, and compression work on the temperature profile. 3) Solution for the case of two particle sizes, yielding the mass flow rate, velocity and temperature profiles of each constituent for a given set of particle loading factors and initial conditions. All the solutions correspond to the following constant parameters:

$$C_{pA} = C_{pB} = 1/(\gamma_0 - 1) = 2.5$$

$$M = 1.3 \qquad Pr = Sc = 1 \qquad C_{pL} = 5$$

Parametric Study

The driving force for the mass transfer is the concentration (or mole fraction) gradient of species B. At the droplet surface, the concentration is determined by the vapor pressure curve of the pure substance. This curve is characterized by two parameters: x_{B0}, the initial mole fraction, and H_{fg}^0, the latent heat of vaporization [see Eq. (9a)]. Calculations were performed for x_{B0} in the range 0.1 to 0.9 and H_{fg}^0 from 2 to 16. Typical values of H_{fg}^0 at room temperature are: Hydrazine, 13; Methyl alcohol, 5.4; Ethyl alcohol, 3.9; n-Hexadecane and n-Dodecane, 3.3; Octane and Freon F11, 1.5. Of course as the critical point of any substance is approached $H_{fg}^0 \to 0$. Through an oversight, water $H_{fg}^0 \cong 22$ was not in the range reported herein. Later calculations confirmed that the character of the relaxation zone is the same for $H_{fg}^0 = 16$ and 22. It was deemed unnecessary to present both results since the nature of our work is only qualitative because of the questionable drag law used.

In addition to x_{B0} and H_{fg}^0, the loading factor δ and the viscosity-radius parameter μ^* were varied. Delta is chosen

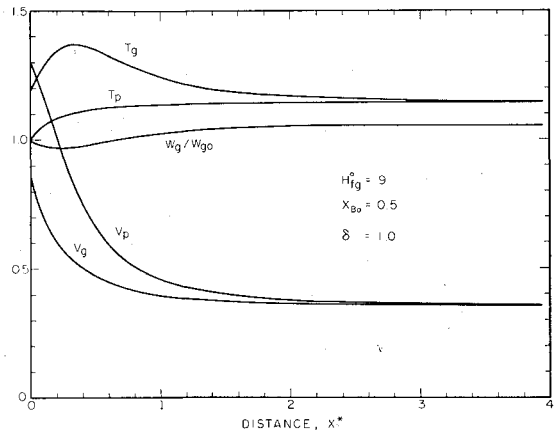

Fig. 2 Typical relaxation zone.

because it has a strong influence upon the solutions, and μ^* because the droplet radius is an important variable from a practical standpoint. The viscosity-radius parameter was computed for oxygen at normal pressure and temperature and allowing for particle sizes from 4- to 100-μ diam.

The primary effect of varying μ^* is on the length of the relaxation zone. In fact, if $C_D \propto Re^{-1}$ and $Nu \propto Re^{1-n}$, then μ^* can be eliminated completely from the problem by defining a new distance variable $X^* = X(\mu^*)^n$. The laws we used were not exactly of this form; nevertheless, the variable $X^* = X(\mu^*)^{1/2}$ yielded results of essentially the same character over the 4- to 100-μ range. Therefore, only results for 4-μ particles are presented here (consult Ref. 10 for the 100-μ curves).

The structure of a typical relaxation zone is given in Fig. 2. The normalized mass flow curve shows that initially the gas condenses and later in the zone the particles vaporize slightly. Note that the gas velocity decreases. This is the result of the "positive friction" of the particles moving faster than the gas. In subsonic flow a positive friction causes a pressure increase, and the temperature rises from the compression work. Subsequent heat transfer to the particles cools the gas.

In the remaining figures, attention is focused upon one variable at a time, thereby emphasizing the effects of the parameters. On each figure, the primary comparison is for different values of the heat of vaporization and the initial mole fraction. Each curve is designated by numbers separated by commas; the first is H_{fg}^0, the second is x_{B0} and the third, if present, is δ.

The mass flow rate of gas is plotted on Fig. 3. All the curves initially decrease, indicating condensation. Curves for $H_{fg}^0 = 16$ all reach a minimum, and, at equilibrium, show a small net vaporization. We see that for $H_{fg}^0 = 16$, the mass transfer is not large irrespective of the other parameters. Situations having large interchanges of mass occur when H_{fg}^0 is low and x_{B0} is high. Then the net effect is condensation of the gas which can lose 80 to 90% of its mass in severe cases. Figure 3 also shows that the relaxation zone thickness decreases as the loading factor δ increases.

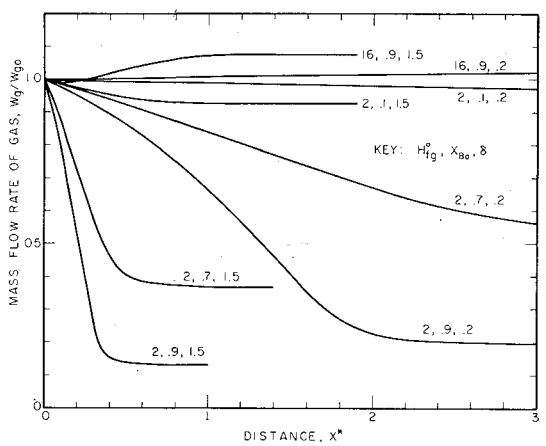

Fig. 3 Parametric study of gas mass flow rate.

Velocities are given on Fig. 4 for loading factors of $\delta = 0.2$ and $\delta = 1.5$, respectively. The relaxation zone is shorter and the final velocities lower for the higher loading factor. The general trends of the curves again demonstrate that low H_{fg}^0 and high x_{B0} produce large mass transfer effects on the relaxation zone.

The temperature curves (Fig. 5) show the most interesting and varied behavior. As noted previously, increasing δ shortens the relaxation zone. Delta also affects the shape of the gas phase temperature curve; increasing δ causes pronounced peaking of the curves and lowers the final equilibrium values. The particle temperature curves are of two different types. When H_{fg}^0 has a high value, the particle temperatures rise quickly to a plateau. This indicates an equilibrium between heating by convection and cooling by evaporation. For low values of H_{fg}^0 the particle temperature rises in a smooth arc to the equilibrium value without establishing this balance. In two cases, the particle temperature exceeds that of the gas which then oscillates before equilibrium is established.

Gas Temperature Investigation

A separate calculation for gas temperature was made in order to verify the computations and gain insight into the

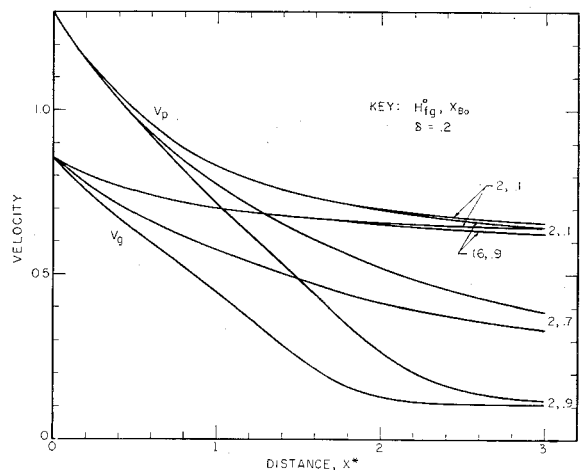

a) Low loading factor

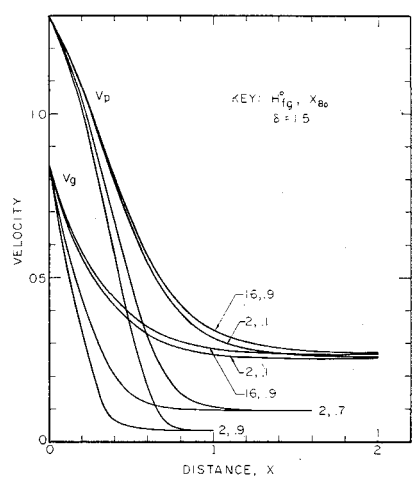

b) High loading factor

Fig. 4 Parametric study of velocities.

behavior. In the previous computations, the gas properties were found from algebraic equations after particle differential equations had been integrated. An alternate method is to integrate a differential equation for the gas temperature itself. This equation is derived by differentiating Eq. (1c) and solving for dH_g/dX. Unwanted derivatives of the particle properties are eliminated using Eqs. (2), while Eqs. (1a) and (1b) are differentiated so that gas phase properties may be substituted for. Utilizing Eqs. (6c–6g) introduces the temperatures. The final steps replace terms containing the mole fractions by employing the derivative of Eq. (7). The result is

$$\frac{d\theta_g}{dX} = \frac{\Psi}{W_g C_p}\left\{C_{pB}(\theta_L - \theta_g) + \frac{1}{2}(V_g - V_p)^2\right\} - \frac{Q}{W_g C_p} + \frac{F}{W_g C_p}(V_g - V_p) + \frac{V_g}{W_g C_p}\frac{dP}{dX} \quad (12)$$

Results of a term-by-term integration of this equation are shown as Figs. 6 and 7. Three cases were chosen from the parametric study, each typical of a different type of temperature curve. One case corresponds to the wavy pattern for low $H_{fg}{}^0$ and x_{B0}, another to the sluggish curves for high $H_{fg}{}^0$ (irrespective of x_{B0}), and the third is typical of the amplified behavior of a high loading factor.

The integral of the first term on the right-hand side of Eq. (12) is the direct influence of the difference in energy between the main gas stream and the gas that is changing phase. In all cases, this term is very small as the thermal and mechanical effects nearly balance. The second term is the contribution by heat transfer, the largest single effect. The heat transfer always gives a negative effect. When the particles are hotter than the gas, the heat transfer changes direction; however, this is only a small contribution. Figure 7a shows

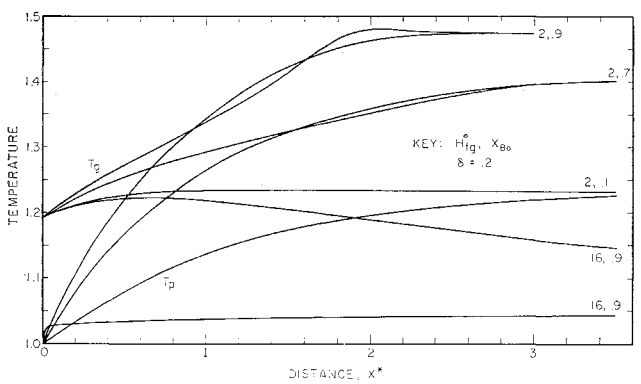

a) Low loading factor

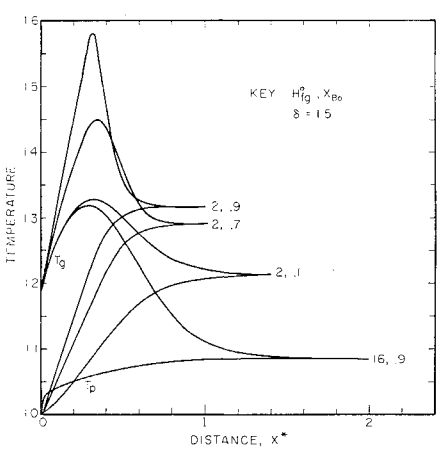

b) High loading factor

Fig. 5 Parametric study of temperatures.

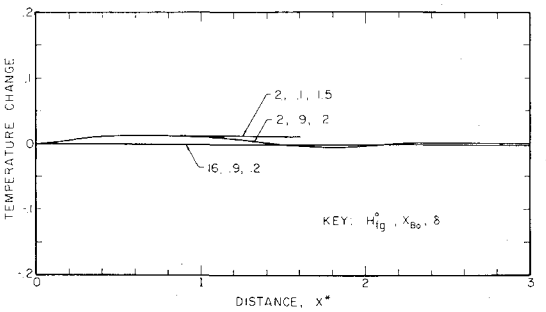

a) Effect of mass transfer

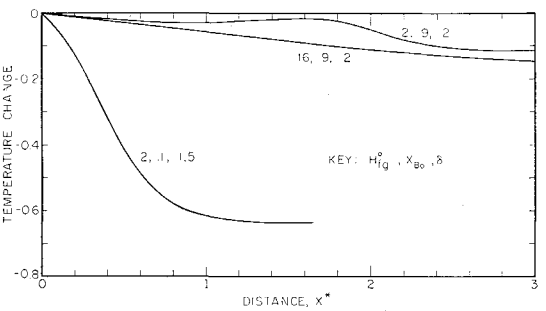

b) Effect of heat transfer

Fig. 6 Gas temperature study.

the drag of the particles upon the gas. For high $H_{fg}{}^0$ this term is negligible; however, for both the other cases it is significant. The effect of compression of the main gas stream is shown in Fig. 7b. All three cases are greatly influenced by this term.

In general, the effect of a high loading factor is to intensify the gas-particle interaction. In the early portion of the relaxation zone, the drag work and gas compression dominate and increase the gas temperature in spite of the heat transferred to the particles. The heat transfer increases as the

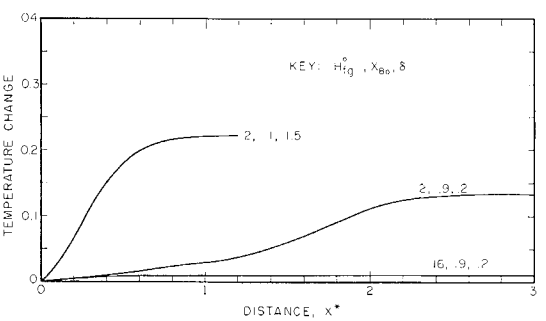

a) Effect of drag work term

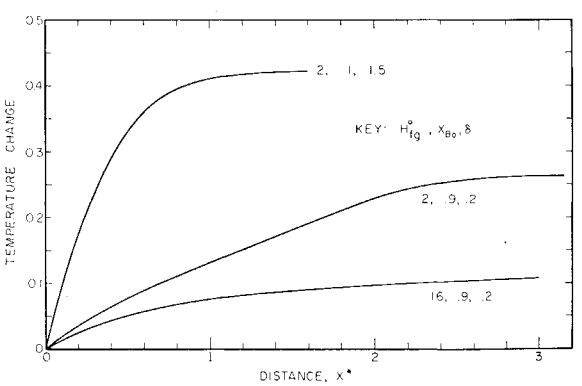

b) Effect of compression work term

Fig. 7 Gas temperature study.

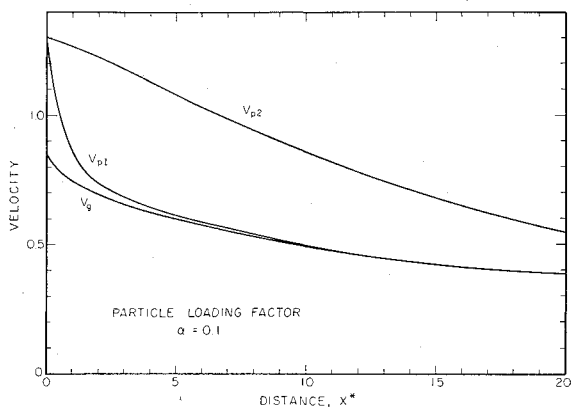

a) Velocities

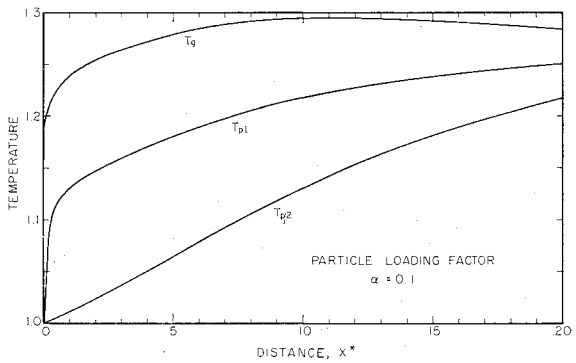

b) Temperatures

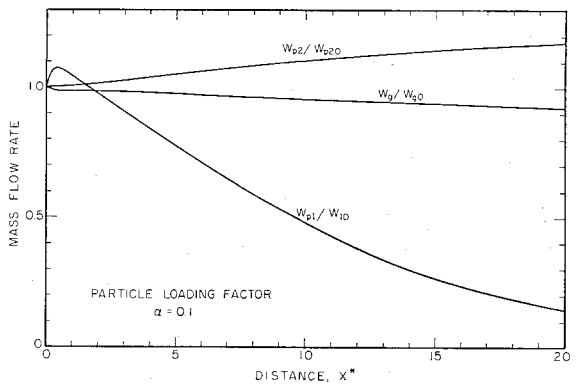

c) Mass flow rates

Fig. 8 Two particle size study.

temperature difference becomes large and finally depresses the temperature in the latter portions of the zone where drag and compression effects decrease. When the mixture contains a small mass of particles, the balance between the mechanical effects and the heat transfer is more delicate.

Consider a small loading and high latent heat H_{fg}^0. The high H_{fg}^0 means that a small change in the liquid temperature results in a large change in the vapor pressure [see Eq. (9a)]. When the particles first pass through the shock, condensation occurs and heat is given up to the particles. Because H_{fg}^0 is high, only a little condensation is needed to increase the particle temperature, but the increased particle temperature results in a very large partial pressure at the particle surface. Thus, condensation gives way to evaporation as the partial pressure at the surface exceeds that in the gas stream. The heat transfer to the particle is completely absorbed by vaporization as the droplet temperature stabilizes. A wet bulb temperature is established in this case. All of this occurs in a short distance behind the shock wave, as shown by the droplet temperature curves. Mechanical effects tend to increase the gas temperature as the vapor is slowly added to the gas, and the heat transfer to the particles slowly decreases the temperature. The approach to equilibrium is very sluggish and the distance required for thermal equilibrium longer than that for the velocity.

Now, when H_{fg}^0 and δ are both small, a completely different temperature curve is observed. The condensation process occurs throughout the relaxation region and the particles do not approach a quasi-steady temperature. Since H_{fg}^0 is small, the partial pressure does not increase much as the particle temperature increases. Therefore, diffusion of vapor to the droplet continues, even for large increases in temperatures. The particle temperature rises from the condensation and the difference between the gas and particle temperature decreases to zero. Thus, the heat transfer changes sign and begins to aid in increasing the gas temperature. It is interesting that here is a situation of heat transfer away from the particles and simultaneous mass transfer to the particle. The heat transfer plays a moderating role as the mechanical effects produce the final equilibrium gas temperature.

Several solutions have been discussed where H_{fg}^0, x_{B0}, and δ were altered. Rudinger presented results for solid particles where he varied the Mach number, the drag law, and the specific heat ratio and found various gas temperature curves. Including these results with ours shows that a wide variety of effects compete to influence the gas temperature, and the final curve is sensitive to changes in a large number of parameters.

Two Particle Sizes

This problem is of interest because spray-producing equipment frequently yields particles in two separate size groups. The initial conditions and constants were not changed from those of the parametric study. In addition, the latent heat H_{fg}^0 was taken as 5, x_{B0} as 0.5, and loading factor δ as unity. There are now two viscosity-radius parameters and these were computed for 4- and 50-μ-diam particles in oxygen at NPT. It is also necessary to introduce group loading factor α as the fraction of particle mass in a size group. The total loading factor δ has its previous meaning.

Results for several cases with different values of α are given in Ref. 10. One case gave a somewhat unexpected result and is presented in Fig. 8. This case is for $\alpha = 0.1$, that is, 10% of the particle mass is small particles.

The gas velocity, Fig. 8a, changes almost entirely because of the interaction with the large particles since they comprise 90% of the particle phase. The small particles approach the gas velocity very rapidly as expected. The temperature curves for the large particles and the gas also behave as one anticipates. The unusual aspect is that the temperature of the small particles does not equilibrate rapidly to the gas temperature. The particle temperature rises rapidly at first but then takes a moderate slope in spite of the velocity equilibrium.

Figure 8c gives the mass flow rates. The large particles grow throughout the relaxation zone. The mass transfer is moderate and the gas mass flow rate shows no significant change. The small particles decrease in mass throughout the relaxation zone until they are almost completely vaporized.

The physical processes for this case are rationalized as follows. A strong interaction of drag work and compression increases the gas temperature. This provides a large heat source for the small particles which increase in temperature and also the vapor pressure. When the surface vapor pressure exceeds that of the gas phase then evaporation begins. There is sufficient heat from the gas to supply the heat of vaporization and increase the particle temperature. The small particles are almost completely vaporized, whereas the large particles are still at a low temperature growing by condensation.

References

[1] Hoenig, S. A., "Acceleration of Dust Particles by Shock Waves," *Journal of Applied Physics*, Vol. 28, 1957, pp. 1218–1219.

[2] Carrier, G. F., "Shock Waves in a Dusty Gas," *Journal of Fluid Mechanics*, Vol. 4, 1958, pp. 376–382.

[3] Rudinger, G., "Some Properties of Shock Relaxation in Gas Flows Carrying Small Particles," *The Physics of Fluids*, Vol. 7, 1964, pp. 658–663.

[4] Kriebel, A. R., "Analysis of Normal Shock Waves in a Particle Laden Gas," *Transactions of the American Society of Mechanical Engineers, Series D: Journal of Basic Engineering*, Vol. 86, 1964, pp. 655–665.

[5] Lu, H. Y. and Chiu, H. H., "Dynamics of Gases Containing Evaporable Liquid Droplets under a Normal Shock," *AIAA Journal*, Vol. 4, No. 6, June 1966, pp. 1008–1011.

[6] Panton, R. L., "Flow Properties for the Continuum Viewpoint of a Nonequilibrium Gas-Particle Mixture," *Journal of Fluid Mechanics*, Vol. 31, 1968, pp. 273–303.

[7] Kliegel, R. B., "Gas Particle Nozzle Flows," *Ninth Symposium (International) on Combustion*, Academic Press, New York, 1963, pp. 811–826.

[8] Rudinger, G., "Experiments on Shock Relaxation in Particle Suspensions in a Gas and Preliminary Determination of Particle Drag Coefficients," *Proceedings of the Symposium on Multiphase Flow*, American Society of Mechanical Engineers, 1963, pp. 55–61.

[9] Bird, R. B., Stewart, W. E., and Lightfoot, E. N., *Transport Phenomena*, Wiley, New York, 1960.

[10] Panton, R. L. and Oppenheim, A. K., "Study of Nonequilibrium Two-Phase Flow of a Gas-Particle Mixture," Rept. AS-66-5, College of Engineering, University of Calif., Berkeley, Calif.

NOVEMBER 1968 AIAA JOURNAL VOL. 6, NO. 11

Experimental Investigation of Laminar Near Wakes behind 20° Wedges at $M_\infty = 6$

RICHARD G. BATT* AND TOSHI KUBOTA†

California Institute of Technology, Pasadena, Calif.

An experimental investigation at $M_\infty = 6$ has been conducted to determine mean-flow properties in near wakes behind several 20° included-angle wedges at zero angle of attack. One cold-wall ($H = 0.3$ in., $T_W/T_0 = 0.19$) and two adiabatic-wall ($H = 0.15$ in., $H = 0.3$ in.) configurations were tested. Freestream Reynolds numbers were varied from 0.5×10^5 to 2×10^5 per in. for each model. Flowfield mappings and flow-property profiles were obtained in the base region for the wedge of 0.3-in. base height with and without cooling by combining Pitot-pressure data with total temperature and mass flux results from hot-wire measurements. The variation of total pressure along streamlines was initially negligible during the shear-layer turning process. Downstream boundaries of these isentropic turns corresponded to viscous-layer edges that were positioned in the outer portions of the shear layers, indicating that wake shocks originated from within viscous regions of the shear layer.

Nomenclature

h = static enthalpy
H = total base height
L = surface distance to trailing edge
M = Mach number
Nu = Nusselt number
p = pressure
p_{t_2} = Pitot pressure
Re = Reynolds number
T = temperature
u = velocity
x = axial distance from model base
y = lateral distance from wake centerline
δ = boundary-layer thickness
θ = wedge included angle
ρ = density
ψ = streamline $\left(= \int_0^y \rho u dy\right)$

Subscripts

aw = adiabatic wall
b = base
C = constant
$\mathfrak{L}$ = centerline
e = edge
N = wake neck
o = reservoir conditions
sp = rear stagnation point
t = local stagnation quantity
TE = trailing edge
W = wall
ws = wedge surface
∞ = freestream

Received January 2, 1968; also presented as Paper 68-99 at the AIAA 6th Aerospace Sciences Meeting, New York, January 22–24, 1968; revision received June 3, 1968. The work discussed in this paper was carried out under the sponsorship and with the financial support of the U.S. Army Research Office and the Advanced Research Projects Agency, Contract DA-31-124-ARO(D)-33. This research is a part of Project DEFENDER sponsored by the Advanced Research Projects Agency.

* Graduate Student, Aeronautics; presently a Member of the Technical Staff at TRW Systems. Member AIAA.

† Associate Professor of Aeronautics. Member AIAA

Introduction

THE near wake behind slender bodies has been the subject of many experimental investigations for the past several years. Both shock-tunnel facilities and continuous-flow wind tunnels have been used for these investigations. Mach numbers ranging from low-supersonic to hypersonic values and flow regimes from all-laminar through transitional to fully developed turbulent flow have been examined. The primary aim has been to determine the basic structure and important scaling parameters for the base regions of hypersonic wakes and thereby define a physically realistic model for the near wake which will be amenable to analytical study. Since many of these previous experimental investigations have been